Inorganic Chemistry

Article

pubs.acs.org/IC

Quantum Chemical Topology Study of the Water-Platinum(II) Interaction

Jacqueline Bergès,*[,†,‡] Isabelle Fourré,[†] Julien Pilmé,[†] and Jiri Kozelka[§,∥]

[†]Laboratoire de Chimie Théorique, UMR 7616 CNRS, Université Pierre et Marie Curie, Sorbonne Universités, Case Courier 137, 4 place Jussieu, 75252 Paris Cedex 05, France

[‡]Université Paris Descartes, 75270 Paris, France

[§]Laboratoire de Chimie et de Biochimie Pharmacologiques et Toxicologiques, Université Paris Descartes, UMR-CNRS 8601, 75270 Paris, France

[∥]Institute of Condensed Matter Physics, Faculty of Science, Masaryk University, Kotlářská 2, 61137 Brno, Czech Republic

Supporting Information

ABSTRACT: The "inverse hydration" of neutral complexes of Pt(II) by an axial water molecule, whose one OH-bond is oriented toward Pt, has been the subject of recent works, theoretical as well as experimental. To study the influence of the ligands on this non-conventional H-bond, we extend here our previous energy calculations, using the second-order Moeller−Plesset perturbation theory (MP2) method together with the Dolg−Pélissier pseudopotential for platinum, to various neutral complexes including the well-known chemotherapeutic agent "cisplatin". The stabilization energy, depending on the nature and the configuration of platinum ligands, is dominated by the same important dispersive component, for all the investigated complexes. For a further characterization of this particular H-bond, we used the atoms in molecules theory (AIM) and the topological analysis of the electron localization function (ELF). The charge transfer occurring from the complex to the water molecule and the Laplacian of the density at the bond critical point between water and Pt are identified as interesting AIM descriptors of this non-conventional H-bond. Beyond this AIM analysis, we show that the polarization of the ELF bonding O−H basin involved in the non-conventional H-bond is enhanced during the approach of the water molecule to the Pt complexes. When the water medium, treated in an implicit solvation model, is taken into account, the interaction energies become independent on the nature and configuration of platinum ligands. However, the topological descriptors remain qualitatively unchanged.

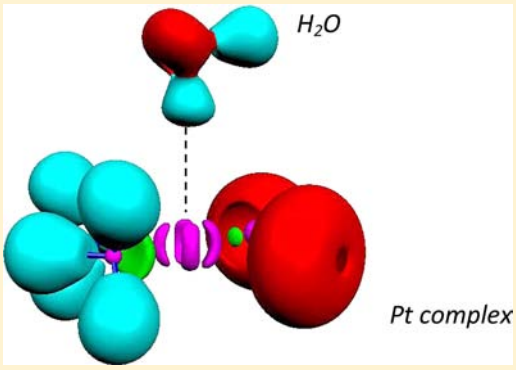

1. INTRODUCTION

The solvation of platinum complexes in water has attracted considerable interest in the past decade from several theoretical and biological points of view. First, a correct description of the solvation shell is of fundamental importance for enabling reliable molecular dynamics (MD) simulations of platinum complexes. Classical MD and Ab Initio Molecular Dynamics (AIMD) simulations of solvated platinum complexes have been instrumental in the evaluation of the structure of platinum-DNA cross-links that are formed by platinum anticancer drugs.[1,2,3] AIMD simulations have been also used for the calculation of ^{195}Pt NMR chemical shifts.[4,5] Second, there has been increasing evidence showing that d^8 ions such as Pt(II) can act as hydrogen bonding acceptor,[1] and, specifically, that water-Pt(II) hydrogen bonding is feasible.[5−8] This finding implies that electrically neutral Pt(II) complexes are hydrated in the "inverse"[9] (or "anionic"[5]) fashion, and suggests that the general view of Pt(II) hydration should be revised. Third, in the cellular processing of the antitumor drug cisplatin, the "inverse hydration" could be the reason for the unexpectedly slow first, rate-determining aquation step.[7] Fourth, for cobalt-dependent methyltransferases, it has been suggested that the "inverse hydration" of the cobalt center could stabilize the Co(I) state and thus help to tune the CoI/II redox potential.[10−12]

Platinum(II) complexes are square-planar, and, in aqueous solutions, water molecules can either approach the platinum atom along the z-axis (perpendicular to the coordination plane), or they can contact the ligands in an in-plane approach. Entries of platinum complex hydrates deposited in the Cambridge Crystallographic Data Centre (CCDC) show both modes of interaction, the ligand contacts being more numerous, as expected from the better accessibility of the ligands with respect to the Pt atom. Nevertheless, 39 structures (as of October 2012) with water molecules placed along the z-axis at a Pt···O distance d of $3.0 \leq d \leq 3.7$ Å could be obtained from the CCDC, in line with our previous second-order Moeller−Plesset perturbation theory (MP2) gas-phase calculations that

Received: July 12, 2012
Published: January 24, 2013

   dx.doi.org/10.1021/ic301512c | *Inorg. Chem.* 2013, 52, 1217−1227

predicted energy minima at similar distances for both neutral and dicationic complexes.[6] As an intermediate between solid hydrates and aqueous solution could be considered crystallized Pt(II)-DNA complexes, which are still solid state structures but are heavily hydrated. Among these, an interesting example is the X-ray structure of a hydrated DNA decanucleotide bearing a (dicationic) interstrand cisplatin cross-link.[13] In that structure, two of the 92 identified water molecules occupy axial positions 3.6 Å below and above the platinum atom. This simultaneous approach of two axial water molecules suggests that in molecular dynamics simulations of solvated Pt(II) complexes the water-Pt(II) interaction must be carefully parametrized. Such a parametrization has been recently attempted using fits to potential energy curves calculated at the MP2 level of theory.[14,15]

Particularly interesting are crystal structures of electrically neutral Pt(II) complexes crystallizing with an axial water molecule, such as *cis*-$[PtBr_2(N\text{-}Gly)_2]\cdot H_2O$[16] or *trans*-$[PtCl_2(NH_3)N\text{-}Gly]\cdot H_2O$.[17] For uncharged Pt(II) complexes interacting with an axial water molecule, MP2 calculations indicated an "H-ahead" approach, where H_2O forms with Pt(II) a non-conventional hydrogen bond.[6,7] For *trans*-$[Pt(OH)_2(NH_3)(gly\text{-}N)]\cdot H_2O$, we recently proved the existence of the O−H···Pt hydrogen-bonding using neutron diffraction.[7]

AIMD calculations have provided arguments for the existence of O−H···Pt hydrogen-bonding even in solution.[5,8,18,19] These calculations were based on density functional theory (DFT), taking profit from the observation that some DFT functionals reproduce, rather surprisingly, relatively well MP2-calculated potential energy curves for the dispersion-driven O−H···Pt interaction.[9,20]

An indirect experimental support for the existence of the O−H···Pt hydrogen-bonding in solution arises from the measurement of the aquation rate constants for cisplatin (*cis*-$[PtCl_2(NH_3)_2]$). This antitumor platinum complex is hydrolyzed in water in two steps, whereby the second aquation would be expected to be considerably lower, because of the impediment of the chloride departure by the positive charge of the monoaquated complex. At variance with this expectation, the two aquation rate constants are found to be nearly equal.[21] This can be interpreted as evidence for the "inverse hydration" of the neutral dichloride form of cisplatin, which orients the axial molecule unfavorably for nucleophilic substitution.

Recently, besides the works about the cisplatin, the role of the nature and position of ligands was studied for some complexes: MD simulations allowed comparing the hydration of the *cis* and *trans* $[PtCl_2(NH_3)_2]$ complexes,[15] and ^{195}Pt NMR calculations investigated the role of the nature of the anionic ligand (X^- = Br^-, Cl^- or OH^-) for *cis*-$[PtX_2(NH_3)_2]$.[5]

The goal of the present work has been a deeper characterization of the non-conventional water-to-Pt(II) hydrogen bonding for several neutral platinum complexes with various polar ligands (chloride and hydroxide) in their *cis* and *trans* configurations, in vacuum as well as in solvent. The implicit solvation model PCM, which was found to reproduce conveniently the explicit solvent (water) effects on the cisplatin and its hydroxido derivatives,[4,5,18,22,23] was used for these platinum complexes in interaction with one axial water molecule.

First, we have examined the impact of the platinum ligands on the interaction energy (section 3.1). Second, we have performed a Quantum Chemical Topology (QCT) analysis of the water-platinum complexes interactions. This allowed us to quantify the charge transfer between the platinum complex and the water molecule, and that between the platinum atom and its ligands, as a function of intermolecular distance (sections 3.2.1, 3.2.2). Third, we have used recent methodological advances[24] employing the electron localization function (ELF), and have analyzed the changes of the dipolar polarization of the O−H σ-bonding pairs in the H-bonding approach as a function of intermolecular distance (section 3.2.3). All these studies were carried out in vacuum and in water.

2. METHODOLOGY

2.1. Sketch of the ELF Quantum Chemical Topology. The Quantum Chemical Topology (QCT)[25,26] may be viewed as a bridge between the picture of the chemical bond derived from the Lewis theory and the first principles quantum-mechanical methods. In a QCT approach, a partitioning of the molecular space into subsystems (basins) is achieved by applying the theory of dynamical systems to a local well-defined function, which should carry the chemical information. The resulting basins are localized around the maxima of the function and are separated by zero flux surfaces. In the Atoms in Molecules theory (AIM) of Bader,[27] the chosen function is the one-electron density $\rho(\mathbf{r})$, and the basins are associated with each of the atoms in the molecule. To characterize the bonding properties in the AIM framework, one uses a series of local indicators among which the values of the density and its Laplacian $\nabla^2\rho_c$, calculated at the bond critical point (BCP). These traditional criteria indicate if the interaction belongs to the closed shell (ρ_c low and $\nabla^2\rho_c$ >0) or to the electron shared interaction (ρ_c large and $\nabla^2\rho_c$ <0). However, more elaborate functions such as the Electronic Localization Function (ELF)[28] can be used. ELF has been interpreted as a signature of the electronic-pair distribution,[29] and its topology provides a partition between core and valence regions.[30] The core basin volumes (if $Z > 2$) are located at nuclear centers and the valence basins (bonding and nonbonding regions) are situated in the remaining molecular space. The valence basins are characterized by the number of core basins with which they share a common boundary. This number is called the synaptic order.[31] Monosynaptic basins (labeled V(A)) correspond to lone pair regions, whereas disynaptic basins (labeled V(A,B)) characterize the covalent bonds. The partition of the molecular space enables basin-related properties to be calculated, by integrating a given density of the property over the volume of the basin, denoted by Ω. For example, the basin populations are defined by $\bar{N}(\Omega) = \int_\Omega \rho(\mathbf{r})\, d\mathbf{r}$.

When dealing with weakly interacting molecular systems, of particular importance are the *deformation* of the interacting basins. A way to compute the basin dipolar polarization vector $\mathbf{M}_1$ components was proposed[32] in the framework of the AIM theory and recently adapted to the ELF topology[24] as follows:

$$M_{1x}(\Omega) = -\int_\Omega (x - X_c)\, \rho(\mathbf{r})\, d\tau$$

$$M_{1y}(\Omega) = -\int_\Omega (y - Y_c)\, \rho(\mathbf{r})\, d\tau$$

$$M_{1z}(\Omega) = -\int_\Omega (z - Z_c)\, \rho(\mathbf{r})\, d\tau$$

where x, y, z are the electronic coordinates and X_c, Y_c, Z_c are the coordinates of the basin center. Because of the invariance of the dipolar polarization magnitude (noted $|\mathbf{M}_1|$) with respect to the orientation of the system of axis, it is then possible to compare the polarization of bonds and lone pairs in different chemical environments. This has shown to be a powerful tool to rationalize the intra- and intermolecular interactions such as the hydrogen bond. In this framework, it has been demonstrated[24] that the molecular dipole is a sum of three contributions as follows:

$$\mu = \sum_\Omega (\mathbf{M}_1(\Omega) - N(\Omega)\mathbf{X}_\Omega) + \sum_\alpha Z\mathbf{X}_\alpha$$

dx.doi.org/10.1021/ic301512c | Inorg. Chem. 2013, 52, 1217−1227

where $\mathbf{M}_1(\Omega)$ is the dipolar polarization of the basin Ω, $\bar{N}(\Omega)$ the basin population, and $\mathbf{X}_\Omega$ is the attractor position of the basin. Z is the atomic number, and $\mathbf{X}_\alpha$ are the nuclear positions of atom α. Each basin dipole (labeled $\mu(\Omega)$) depends of the orientation of the system of axes, but their sums over all basins system (molecular dipole μ) do not depend of the axis orientation for a neutral system. Thus, in the AIM framework, the dipole of the water molecule (labeled μ_{H2O}) can be calculated as the sum of each dipole atomic contributions in a common axis system situated on the oxygen atom, as follows:

$$\begin{aligned}\mu_{H2O} &= \mu(O) + \mu(H_1) + \mu(H_2)\\ &= \mathbf{M}_1(O) + \mathbf{M}_1(H_1) + \mathbf{M}_1(H_2) + [Z(O) - \bar{N}(O)]\mathbf{X}_O\\ &\quad + [(Z(H_1) - \bar{N}(H_1)]\mathbf{X}_{H_1} + [Z(H_2) - \bar{N}(H_2)]\mathbf{X}_{H_2}\\ &= \mathbf{M}_1(O) + \mathbf{M}_1(H_1) + \mathbf{M}_1(H_2) + q_O\mathbf{X}_O + q_{H_1}\mathbf{X}_{H1}\\ &\quad + q_{H_2}\mathbf{X}_{H2}\end{aligned}$$

Here $\mathbf{X}_O$, $\mathbf{X}_{H1}$, and $\mathbf{X}_{H2}$ are the nuclear positions, and q_O, q_{H1}, and q_{H2} are the atomic charges of oxygen and hydrogen atoms respectively. Thus, the whole charge of the water molecule is expressed as $q_{H2O} = q_O + q_{H1} + q_{H2}$.

2.2. Computational Methods. The interaction energies between each Pt-complex and one axial water molecule were evaluated, at MP2 and Hartree–Fock (HF) levels of theory, as the difference between the total energy of the two interacting species, corrected for the basis set superposition error (BSSE) using the Counterpoise method[33,34] and the sum of the total energies of the individual molecules. The all-electron 6-311+G(2d,2p) basis sets were used for the H, N, O, and Cl atoms, whereas for Pt, we used the Dolg–Pélissier pseudopotential/pseudoorbital basis set including two polarization f orbitals.[35,36] The MP2 calculations using these orbital bases were shown to reproduce satisfactorily the geometries and dipole moments of platinum complexes.[36] As in previous work,[6,9,37] we related the difference $\Delta E_{MP2} - \Delta E_{HF}$ to the dispersion contribution to the interaction energy. Although the difference $\Delta E_{MP2} - \Delta E_{HF}$ contains also the correlation contribution to the intramolecular electrostatic and induction energy, and exchange-correlation effects,[38] in many cases, the dispersion effect is dominant.[39]

Solvation effects on the interaction energies and topological analysis were accounted for with the COSMO option for the Polarized Continuum Model CPCM, the dielectric constant being the one of water, that is, $\varepsilon = 78.39$. Some calculations were also performed with IEFPCM that gave identical results. The CPCM models are well adapted to calculate the solvation energies of isolated platinum complexes.[5] However they should be used with caution to describe the intermolecular weakly bonded interaction between the complex and the axial water molecule. It must be noted that our purpose was to derive trends of the influence of the aqueous medium on the characteristics of these intermolecular H-bonds.

All energy calculations were carried out using the Gaussian03 and Gaussian09 suites of programs.[40] The interaction energies in the solvent were calculated without the BSSE correction. Topological analysis of the electron density field and of the electron localization function (populations, atomic charges, and dipolar moments) were performed at the MP2[29] level by means of the TopChem90 package,[24,41,42] a modified version of the TopMod package.[43] A parallelepipedic box grid of points, with a step size of 0.08 bohr, was used. The ELF isosurfaces were visualized with the Molekel 4.3 software.[44]

3. RESULTS AND DISCUSSION

3.1. Interaction Energies between the Pt Complexes and One Water Molecule. For the five electrically neutral platinum complexes, **1** *cis*-$[PtCl_2(NH_3)_2]$, **2** *trans*-$[PtCl_2(NH_3)_2]$, **3** *cis*-$[Pt(OH)_2(NH_3)_2]$, **4** *trans*-$[Pt(OH)_2(NH_3)_2]$, and **5** *trans*-$[PtCl_2(NH_3)N\text{-}Gly]$, we have considered the interaction with an axial water molecule, as shown in Figure 1. The water molecule was oriented toward platinum by one of the O–H bonds (hydrogen-bonding or "H-ahead" orientation, Figure 1a) or by one of its lone-pairs (classical coordination or "lone pair-ahead" orientation, Figure 1b).

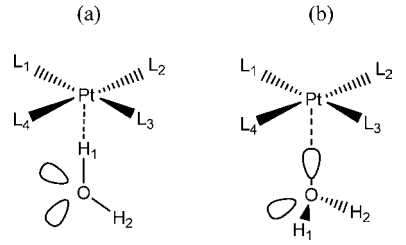

Figure 1. Pt complexes in (a) the "H-ahead orientation" and (b) the "lone pair-ahead" orientation. The ligands are as follows, for compound **1**, $L_1 = L_2 = Cl^-$, $L_3 = L_4 = NH_3$; for **2**, $L_1 = L_3 = Cl^-$, $L_2 = L_4 = NH_3$; for **3**, $L_1 = L_2 = OH^-$, $L_3 = L_4 = NH_3$; for **4**, $L_1 = L_3 = OH^-$, $L_2 = L_4 = NH_3$; for **5**, $L_1 = L_3 = Cl^-$, $L_2 = NH_3$, $L_4 = NHCH_2COOH$. The geometrical parameters to be considered are the Pt–O distance and the dihedral angle $\theta = H_2\text{–}O\text{–}Pt\text{–}L_1$ (to be optimized at each step of the scan along the Pt–O distance).

For both orientations, we considered a number of discrete Pt–O distances at which the two partner molecules (the platinum complex and H_2O) were placed. Both molecules were kept frozen in their individually optimized geometries, a common practice used in previous studies.[6,7,14,15,18,20,45] Neglecting nuclear relaxation seemed justified, as judged from our previously performed calculation for the "H-ahead" approach of *trans*-$[Pt(OH)_2(NH_3)_2]$ for which a stabilization by full relaxation of only 0.05 kcal.mol^{-1} was found.[6] We kept the axial orientation of the water molecule along the scans, the dihedral angle θ (H_2–O-Pt-L_1) being optimized at each d(Pt–O) value (see Figure 1).

The interaction energy curves obtained at the HF and MP2 levels, for one axial water molecule interacting with *cis*- and *trans*-$[PtX_2(NH_3)_2]$ (X= Cl and OH) in the "H-ahead" approach, are shown in Figure 2. The curves for *trans*-$[PtCl_2(NH_3)N\text{-}Gly]$ were published previously.[7] Table 1 lists numerical values of the interaction energies ΔE at discrete O···Pt distances. It can be seen that for all the complexes, the MP2 equilibrium O···Pt distance is identical (~3.4 Å), but the equilibrium interaction energy depends somewhat (i) on their nature and (ii) on their position (*cis* and *trans* isomerism). We included also in Table 1 values of the interaction energies without the counterpoise correction for the equilibrium distances. As it can be seen, the basis set superposition errors are relatively large.[46]

First, the interaction energy is slightly larger (more stabilizing by 1,5 kal/mol) for the hydroxido complexes, as compared with the chlorido complexes (both in the *cis* and the *trans* configuration). Second, the interaction with the water molecule appears reinforced in the *cis* configuration. This seems related to the orientation of the OH bond of water not directed toward platinum, with respect to the anionic ligands X^- (X = Cl or OH). For the *cis*-$[PtX_2(NH_3)_2]$ complexes, the dihedral angle θ (Figure 1) remained equal to 45° all along the scan (i.e., OH located in the plane bisecting the X-Pt-X angle), whereas for the *trans*- complexes the optimized θ value was 0° throughout (OH located above the polar Pt-X bond). In other words the water molecule rotates about the Pt···H–O axis so as to

dx.doi.org/10.1021/ic301512c | Inorg. Chem. 2013, 52, 1217–1227

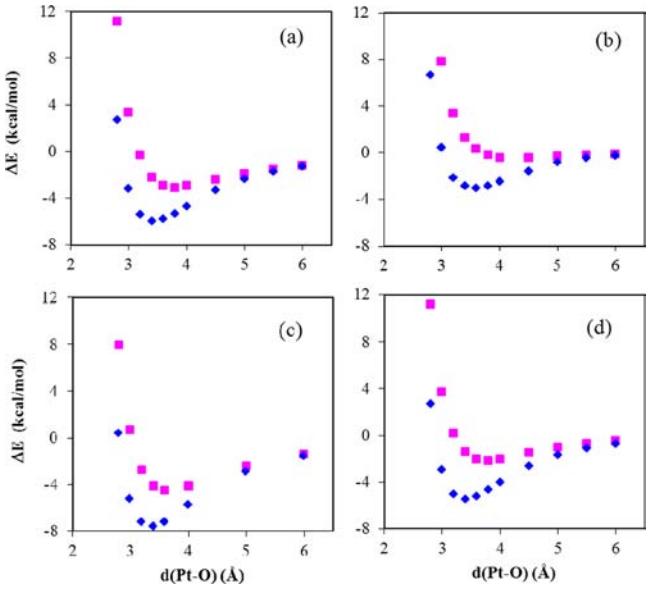

Figure 2. Interaction energy, corrected for the basis set superposition error (BSSE), ΔE, at the Hartree–Fock (pink symbols) and at the MP2 levels (blue symbols) in the "H-ahead" orientation for (a) *cis*-$[PtCl_2(NH_3)_2]\cdot H_2O$, (b) *trans*-$[PtCl_2(NH_3)_2]\cdot H_2O$, (c) *cis*-$[Pt(OH)_2(NH_3)_2]\cdot H_2O$, and (d) *trans*-$[Pt(OH)_2(NH_3)_2]\cdot H_2O$.

Table 1. Interaction Energies of the Pt-Complexes with H_2O in the "H-ahead" Orientation, for Selective Distances between Platinum and the Oxygen Atom of the Water Molecule[a]

compd	d(Pt–O)	ΔE[b]	ΔE_{sol}[c]
cis-$[PtCl_2(NH_3)_2]\cdot H_2O$	2.4	46.9	44.9
	3.0	−3.2	−1.9
	3.4	***−6.0*** *(−8.0)*	***−4.2***
	6.0	−1.3	−0.4
trans-$[PtCl_2(NH_3)_2]\cdot H_2O$	2.4	49.2	44.4
	3.0	−1.1	−2.1
	3.4	***−4.1*** *(−6.1)*	***−4.2***
	6.0	−0.5	−0.4
cis-$[Pt(OH)_2(NH_3)_2]\cdot H_2O$	2.4	44.0	43.5
	3.0	−5.2	−2.5
	3.4	***−7.6*** *(−9.2)*	***−4.4***
	6.0	−1.5	−0.3
trans-$[Pt(OH)_2(NH_3)_2]\cdot H_2O$	2.4	46.2	42.1
	3.0	−3.0	−2.5
	3.4	***−5.5*** *(−7.2)*	***−4.0***
	6.0	−0.8	−0.2
trans-$[PtCl_2(NH_3)$ *N-Gly*$]\cdot H_2O$	2.4	50.0	
	3.0	−0.4	
	3.4	***−3.9*** *(−6.1)*	
	6.0	0.3	

[a] d(Pt–O) is in Å, ΔE calculated at the MP2 level is in kcal/mol. [b] ΔE is defined as the energy including BSSE of the following reaction: [Pt-complex]$\cdot H_2O \rightarrow$ [Pt-complex] + H_2O. [c] ΔE_{sol} is calculated without BSSE. Values in italics correspond to the energy minima, those in parentheses being obtained without BSSE.

maximize the attraction between the proton of the non-interacting OH bond with the anionic ligand(s).

The HF curves for the "H-ahead" interactions of the complexes *cis*-$[PtCl_2(NH_3)_2]$, *cis*-$[Pt(OH)_2(NH_3)_2]$, and *trans*-$[Pt(OH)_2(NH_3)_2]$ show a shallow minimum between 3.8 and 4 Å, whereas for *trans*-$[PtCl_2(NH_3)$N-*Gly*$]$ and *trans*-$[PtCl_2(NH_3)_2]$, the HF curves do not show any minimum at all. We conclude that the shallow minimum seen in the three former cases is of electrostatic origin and is related to the water-ligand interactions discussed above. Importantly, at the Pt···O distance corresponding to the MP2 energy minimum, the difference between the MP2 and HF interaction energies, $\Delta E_{MP2} - \Delta E_{HF}$, is very similar for all five "H-ahead" complexes, indicating that the dispersion component is crucial for the stabilization of the H-bonding approach.[6,7]

We also studied the effect of solvation on the "inverse" hydration (i.e., the "H-ahead" approach), using a continuum model (see Section 2.2). As it can be seen from Table 1, the equilibrium O···Pt distances are identical to those obtained in vacuum, but the stabilization energy is now practically independent of the nature and configuration of the platinum ligands. Thus, the interaction energy becomes uniform, amounting approximately to −4 kcal/mol. This supports our view that the differences seen in the "in vacuo" calculations between the different platinum complexes are mainly due to electrostatic/hydrogen bonding interactions between the non-interacting O–H bond and the platinum ligands. The screening effect of the solvating water molecules seems to make these interactions relatively unimportant. However, one has to be careful with interpreting calculations using the implicit solvation model. The damping effect of the ligand-axial water interactions by solvent screening may not be as complete as our calculations indicate. To overcome this effect we performed calculations with various Pt radii as it was successfully envisaged for isolated platinum,[5] but no drastic change has been observed in the energies.

The "lone pair-ahead" approach is repulsive for all complexes (for instance see Supporting Information, Figure S1), in agreement with previous calculations.[6,7]

We can conclude from the interaction energy calculations that for the "inverse" hydration" of the neutral complexes, the principal component of the favorable "H-ahead" interaction, the dispersion component, is apparently independent of the platinum ligands. The platinum ligands affect the interaction energy mainly by electrostatic forces with the non-interacting O–H bond of the axial water molecule; these interactions are however effectively screened by the solvating shell of water molecules.

In the following section we will explore the capacity of topological approaches to provide new insights in the bonding of H_2O with platinum complexes.

3.2. Topological Characterization of the H_2O–Pt Complexes Interaction. *3.2.1. AIM Analysis.* We have used the AIM formalism to determine the charges on the platinum atom, on each ligand, and on the axial water molecule. Table 2 presents these charges for both approaches of the water molecule to the platinum complexes **1**–**5**, for selected Pt–O distances. The charge of the central atom varies noticeably from 0.60 e to ∼0.85 e, the larger values being observed with the OH^- ligands.

Regarding the electron transfer from the ligands to the central Pt atom, Table 2 shows that the anionic ligands donate more electrons to platinum (0.4–0.6 e) than do the neutral ligands (0.2–0.3 e), as expected. Moreover, the chloride anion donates more electrons to platinum (around 0.5 e) than does the hydroxide ligand (around 0.4 e), which is in agreement with the respective electronegativity of the oxygen and the chlorine atoms.

dx.doi.org/10.1021/ic301512c | *Inorg. Chem.* 2013, 52, 1217–1227

Table 2. QTAIM Charge Analysis: Net Atomic Charges q[a] of the Platinum Center, the Ligands, and the Water Molecule, for the Pt-Complexes in Interaction with H_2O[b,c]

		QTAIM charges					
	d(Pt−O)	Pt	Cl	OH	N-*Gly*	NH_3	H_2O
			"H-ahead"				
cis-$[PtCl_2(NH_3)_2]\cdot H_2O$	2.4	0.65	−0.50			0.24	−0.13
	3.0	0.61	−0.50			0.24	−0.08
	3.4	*0.60*	*−0.51*			*0.24*	*−0.04*
	6.0	0.60	−0.52			0.22	0.00
trans-$[PtCl_2(NH_3)_2]\cdot H_2O$	2.4	0.64	−0.53			0.27	−0.13
	3.0	0.61	−0.53			0.26	−0.06
	3.4	*0.60*	*−0.53*			*0.26*	*−0.04*
	6.0	0.60	−0.55			0.26	0.01
cis-$[Pt(OH)_2(NH_3)_2]\cdot H_2O$	2.4	0.80		−0.55		0.22	−0.14
	3.0	0.76		−0.57		0.23	−0.08
	3.4	*0.75*		*−0.56*		*0.21*	*−0.05*
	6.0	0.74		−0.57		0.20	0.00
trans-$[Pt(OH)_2(NH_3)_2]\cdot H_2O$	2.4	0.82		−0.60		0.26	−0.13
	3.0	0.79		−0.60		0.24	−0.07
	3.4	*0.78*		*−0.61*		*0.24*	*−0.04*
	6.0	0.77		−0.61		0.23	0.00
trans-$[PtCl_2(NH_3)$N-*Gly*$]\cdot H_2O$	2.4	0.68	−0.53		0.25	0.24	−0.13
	3.0	0.66	−0.54		0.25	0.23	−0.08
	3.4	*0.65*	*−0.54*		*0.24*	*0.23*	*−0.04*
	6.0	0.69	−0.55		0.21	0.20	0.00
			"lone pair-ahead"				
cis-$[PtCl_2(NH_3)_2]\cdot H_2O$	2.4	0.65	−0.53			0.21	−0.01
	3.4	0.62	−0.52			0.22	−0.01
	6.0	0.58	−0.51			0.23	0.00
trans-$[PtCl_2(NH_3)_2]\cdot H_2O$	2.4	0.68	−0.58			0.24	0.00
	3.4	0.64	−0.56			0.24	0.00
	6.0	0.61	−0.55			0.24	−0.01
cis-$[Pt(OH)_2(NH_3)_2]\cdot H_2O$	2.4	0.82		−0.60		0.20	−0.02
	3.4	0.79		−0.59		0.20	−0.01
	6.0	0.74		−0.58		0.21	0.00
trans-$[Pt(OH)_2(NH_3)_2]\cdot H_2O$	2.4	0.83		−0.63		0.22	−0.01
	3.4	0.80		−0.62		0.22	−0.02
	6.0	0.77		−0.61		0.23	0.00
trans-$[PtCl_2(NH_3)$N-*Gly*$]\cdot H_2O$	2.4	0.71	−0.57		0.23	0.21	−0.01
	3.4	0.68	−0.56		0.23	0.24	0.00
	6.0	0.71	−0.55		0.20	0.21	0.01

[a]In electron. [b]Values in italics correspond to the Pt−O equilibrium distances. "H-ahead" (respectively "lone pair-ahead") means that one H atom (respectively one lone pair) of the water molecule points towards the platinum. [c]The net atomic charges q are calculated in the following way: For a ligand X (X = Cl, NH_3, OH, H_2O), $q(X) = \sum_{atoms} Z_X\,(atom) - \overline{N_X}\,(atom)$ where $Z_X(atom)$ is the atomic number of a particular atom of X, and $\overline{N_X}\,(atom)$ is the integrated density in the corresponding atomic basin (AIM population). For Pt, $q(Pt) = 18 - \overline{N}(Pt)$.

Regarding the charge transfer from the platinum complex to the water molecule, we observe different behavior for the "H-ahead" versus the "lone pair-ahead" approaches. In the "H-ahead" orientation, whatever the complex, an increase of negative charge on the water molecule is observed when the two partners approach, amounting to −0.04 e at the equilibrium O···Pt distance of 3.4 Å and reaching −0.13 e at 2.4 Å (Table 2).

We also note that for the "H-ahead" approach, the charge transfer from ligands to platinum increases as d(Pt−O) decreases, in synergy with the charge transfer from the platinum complex to water. This transfer correlates with an increase of the dipole moment of H_2O (μ_{H2O}). Indeed, μ_{H2O} remains almost constant up to the equilibrium distance, that is, in a range of distances where the charge transfer is very small (μ_{H2O} = 1.97 D for *trans*-$[PtCl_2(NH_3)_2]$ at d(Pt−O) = 3.4 Å). For d(Pt−O) < 3.4 Å, μ_{H2O} increases (μ_{H2O} = 2.24 D at 2.4 Å), concomitantly with the charge transfer, thus documenting the fact that the local dipole moment of H_2O in the "H-ahead" approach is related to the charge transfer.

In contrast to the "H-ahead" approach, Table 2 shows that in the "lone pair-ahead" orientation, the charge transfer from Pt to the water molecule remains zero within error limits down to O···Pt = 2.4 Å, suggesting that down to this distance, the orbital overlap remains negligible. At variance with the "H-ahead" approach, in the "O-ahead" approach, the charge transfer from the ligands to platinum decreases. This is in agreement with the lone pair of oxygen repelling the Pt-X bonding electrons from platinum. The value of μ_{H2O} remains close to the value calculated for the isolated water molecule (1.97 D) for Pt−O > 3.0 Å, whatever the considered system. Below 3.0 Å, the μ_{H2O} value decreases, reaching 1.71 D at 2.4 Å, which suggests a

dx.doi.org/10.1021/ic301512c | Inorg. Chem. 2013, 52, 1217−1227

Table 3. QTAIM Charge Analysis for the "H-ahead" Interaction of the $[PtX_2(NH_3)_2]$ Complexes (X = Cl, OH), in Their *cis* and *trans* Geometries, Taking into Account Implicit Solvation in Water (See Text)[a]

		QTAIM charges				
	d(Pt−O)	Pt	Cl	OH	NH_3	H_2O
cis-$[PtCl_2(NH_3)_2]\cdot H_2O$	2.4	0.71	−0.58		0.30	−0.14
	3.0	0.67	−0.59		0.29	−0.07
	3.4	*0.66*	*−0.60*		*0.29*	*−0.05*
	6.0	0.65	−0.61		0.28	0.00
trans-$[PtCl_2(NH_3)_2]\cdot H_2O$	2.4	0.69	−0.57		0.29	−0.14
	3.0	0.65	−0.58		0.29	−0.07
	3.4	*0.64*	*−0.58*		*0.29*	*−0.05*
	6.0	0.63	−0.60		0.28	0.00
cis-$[Pt(OH)_2(NH_3)_2]\cdot H_2O$	2.4	0.84		−0.64	0.30	−0.16
	3.0	0.80		−0.66	0.30	−0.08
	3.4	*0.78*		*−0.64*	*0.28*	*−0.05*
	6.0	0.78		−0.66	0.27	0.00
trans-$[Pt(OH)_2(NH_3)_2]\cdot H_2O$	2.4	0.83		−0.63	0.29	−0.13
	3.0	0.80		−0.63	0.29	−0.09
	3.4	*0.78*		*−0.64*	*0.27*	*−0.05*
	6.0	0.77		−0.64	0.27	0.00

[a]See Table 1 for the details on each entry.

Table 4. Properties of the Bond Critical Point (BCP) between the Pt-Complex and the Water Molecule in the "H-ahead" Orientation: Charge Density ρ_c, Laplacian $\nabla^2\rho_c$ for Selective Distances d(Pt−O)[a]

				$\nabla^2\rho_c$	
compound	d(Pt−O)	x_c	ρ_c	vacuum	water
cis-$[PtCl_2(NH_3)_2]\cdot H_2O$	2.4	0.222	0.185	**0.085**	0.051
	2.8	0.293	0.074	**0.119**	0.118
	3.0	0.294	0.047	**0.085**	0.082
	3.4	*0.316*	*0.020*	***0.047***	*0.046*
	3.6	0.322	0.013	**0.035**	0.034
trans-$[PtCl_2(NH_3)_2]\cdot H_2O$	2.4	0.222	0.185	**0.082**	0.051
	2.8	0.293	0.076	**0.115**	0.118
	3.0	0.294	0.047	**0.085**	0.082
	3.4	*0.316*	*0.020*	***0.047***	*0.046*
	3.6	0.322	0.013	**0.035**	0.035
cis-$[Pt(OH)_2(NH_3)_2]\cdot H_2O$	2.4	0.222	0.186	**0.070**	0.039
	2.8	0.293	0.072	**0.125**	0.112
	3.0	0.294	0.047	**0.081**	0.078
	3.4	*0.316*	*0.020*	***0.045***	*0.044*
	3.6	0.322	0.013	**0.034**	0.034
trans-$[Pt(OH)_2(NH_3)_2]\cdot H_2O$	2.8	0.293	0.072	**0.125**	0.108
	3.0	0.294	0.047	**0.081**	0.078
	3.4	*0.316*	*0.020*	***0.045***	*0.044*
	3.6	0.322	0.013	**0.034**	0.034

[a]Also given is the location of the BCP as a fraction of the Pt−H distance ($x_C = d$(H-BCP)/d(Pt−H) with d(Pt−H) = d(Pt−O) − 0.958 Å). Charge densities and Laplacians are in a.u. and distances are in Å. Values in italics are associated to the Pt−O equilibrium distances. All the quantities given in the table have been obtained in vacuum. The $\nabla^2\rho_c$ values in water were also reported.

delocalization of the density from oxygen lone pair basins toward O−H because of repulsive effects.

Taken into account the small extent of charge transfer that we observe for the "H-ahead" approach at equilibrium distance (0.04 e), one could ask whether the difference from the complete absence of charge transfer observed for the "O-ahead" approach is significant. However, it is well-known that the charge transfer in hydrogen bonded systems is very low, from a few to 50 millielectrons.[47] For example, in the prototypical example for H-bonding, the water dimer, the charge transfer has been calculated to amount only 0.02 e.[48] In this context, the 0.04 e charge transfer calculated for Pt-complexes in the "H-ahead" orientation appears as a non-negligible value. Furthermore, beyond the equilibrium distance, the charge transfer increases considerably in the "H-ahead" approach, proving that we are dealing with a real orbital overlap phenomenon, whereas for the "O-ahead" approach, the water-to-platinum charge transfer remains strictly absent down to O···Pt = 2.4 Å. Finally, additional support for platinum-to-water charge transfer being a significant marker of the "H-ahead" approach arises from a recent study of the nature of HO−H···Pt interaction in the *trans*-$[PtCl_2(NH_3)(N\text{-Gly})]\cdot H_2O$ complex.[49] The authors used several AIM criteria[50] and a Natural Bond Orbital analysis[51] to characterize the complex as a

dx.doi.org/10.1021/ic301512c | Inorg. Chem. 2013, 52, 1217−1227

closed-shell interaction with a small charge transfer from platinum to water. We therefore believe that the water-to-platinum charge transfer, although probably contributing only a small amount of the interaction energy, is a significant and interesting descriptor of the "H-ahead" approach. Our results suggest that in the "H-ahead" approach, there is, at equilibrium distance, a small but detectable orbital overlap, which is not the case in the "O-ahead" approach.

Conversely to what was observed for the interaction energies, including the solvent effects does not change dramatically the conclusions drawn above. Interestingly, in the "H-ahead" orientation, the transfer from the ligands to the platinum slightly decreases, whereas the transfer from the platinum to the water molecule remains nearly unchanged, whatever the Pt−O distance (Table 3). The consequence is that the net charge of the metal atom is enhanced with respect to the one in vacuum, to a greater extent for $[PtCl_2(NH_3)_2]$ than for $[Pt(OH)_2(NH_3)_2]$.

Analysis of the Laplacian of the density field at the critical point between the water molecule and the Pt-complex in the "H-ahead" orientation allows one to obtain a deeper insight into the peculiar inverse H-bond beyond a charge analysis (Table 4). For all the considered Pt-complexes, at the equilibrium Pt−O distance, the density at the bond critical point and its Laplacian ($\rho_c \approx 0.020$ and $\nabla^2\rho_c \approx 0.045$ au) are within the appropriate range for the hydrogen bond[52] (i.e., [0.002, 0.04] a.u. for ρ_c and [0.02, 0.15] a.u. for $\nabla^2\rho_c$), and are of the same order of magnitude than in previously published works.[20,47] When the water molecule approaches platinum, both ρ_c and $\nabla^2\rho_c$ increase, in agreement with increasing orbital overlap.

A maximum is reached for $\nabla^2\rho_c$ between 2.4 and 3.0 Å, higher for $[Pt(OH)_2(NH_3)_2]$ than for $[Pt(Cl)_2(NH_3)_2]$ which indicates a greater concentration of charge at the BCP. This could be related to the greater AIM charge of the Pt atom (Table 2). At very short distances (under 3.0 Å), ρ_c continue to increase whereas $\nabla^2\rho_c$ starts to decrease and the critical point gets closer to the H atom. These findings are in agreement with several studies of AIM descriptors in hydrogen bonded dimers as a function of the intermolecular distances.[53,54] In water, the variations of $\nabla^2\rho_c$ as a function of the water-complex distance are essentially the same as in vacuum (the position of the critical point and the density being unchanged), with some discrepancies at short distances.

3.2.2. ELF Local Dipolar Polarization M_1. Figure 3 displays the ELF = 0.80 localization domains of the complex *cis*-$[PtCl_2(NH_3)_2]\cdot H_2O$ in the "H-ahead" approach at two different Pt−O distances (3.4 and 2.4 Å). Consistently with a closed-shell interaction picture, no bonding basin was found between the complex and the water molecule, whatever the Pt−O distance. Thus, the topology of the water molecule in the complex remains identical to the one of the isolated molecule: it is composed of the core basin of oxygen C(O), two bonding basins associated with the O−H bonds (pointing toward Pt and $V(O,H_2)$) as well as two nonbonding basins associated with the oxygen lone pairs ($V_i(O)_{i=1,2}$), distributed in a tetrahedral arrangement around C(O) in agreement with the valence shell electron pair repulsion (VSEPR) model.[55]

It is noteworthy that summing up the $V(O,H_i)_{i=1,2}$ and $V_i(O)_{i=1,2}$ populations allows recovering the global charge transfer obtained in the AIM framework (section 3.2.1). However, since this extra charge density is shared between several basins, the variation of population of each specific basin

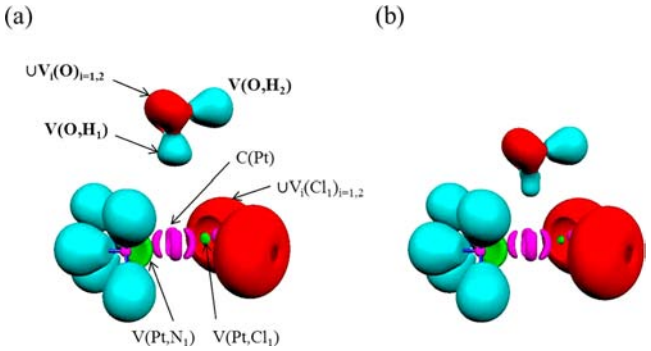

Figure 3. ELF = 0.80 isosurfaces of the *cis*-$[PtCl_2(NH_3)_2]\cdot H_2O$ complex in the "H-ahead" orientation for (a) d(Pt−O) = 3.4 Å and (b) d(Pt−O) = 2.4 Å. The valence basins of the water molecule are indicated by arrows, as well as some core and valence basins of the complex. For this value of ELF, the two lone pair basins of the oxygen of water are not yet separated, as well as the lone pairs of the chlorine atom.

can be very small.[54] Indeed, the $V(O,H_i)_{i=1,2}$ and $V_i(O)_{i=1,2}$ populations remain close to the values obtained for the isolated molecule (1.68 e for V(O,H) and 2.27 e for V(O)) as d(Pt−O) decreases from 6.0 to 3.0 Å (Supporting Information, Table S1). Obviously, this is not true anymore for very short distances (as 2.4 Å), specifically for the "H-ahead" approach for which a non-negligible charge transfer occurs. Whereas the $V(O,H_2)$ population remains approximately constant, the extra charge density is redistributed among the lone pair basins, the $V(O,H_1)$ population even slightly decreasing.

The variations of the $V(O,H_1)$ population as a function of d(Pt−O) is too low to provide reliable descriptors of this peculiar interaction. However, in agreement with a previous work dealing with $[Pt(H_2O)_4]^{2+}$ in interaction with an axial water molecule,[18] a contraction of the interacting $V(O,H_1)$ localization domain is observed at the equilibrium distance (Figure 3a). This contraction is more obvious at short distance (where it is also associated to a strong modification of the shape, Figure 3b), probably because of repulsive interactions. In an attempt to extract a topological signature from the $V(O,H_1)$ distortion, the spatial distribution of the electron density in the ELF basin volumes of the water molecule was thus analyzed by means of local dipolar polarizations $|\mathbf{M}_1|$.[24] In Table 5 are reported the $|\mathbf{M}_1|$ values of the basins associated with the O−H bonds ($V(O,H_i)_{i=1,2}$) and the lone-pairs ($V_{i=1,2}(O)$) for selected Pt−O distances between 2.4 and 6.0 Å of the compounds **1** to **5**. Figure 4 displays the $|\mathbf{M}_1|$ variations for *cis*- and *trans*-$[Pt(X)_2(NH_3)_2]\cdot H_2O$, X = Cl, NH_3, whereas those associated to *trans*-$[PtCl_2(NH_3)Gly]\cdot H_2O$ are shown in Supporting Information, Figure S2.

At long Pt···O distances (from 6.0 up to about 4.5 Å), the $|\mathbf{M}_1|$ values of the interacting and non-interacting O−H bonds (i.e., of the $V(O,H_1)$ and $V(O,H_2)$ basins) are close to their value in free H_2O (0.79 au). Similarly, the $|\mathbf{M}_1|$ values of the lone pairs at long d(Pt−O) distances are close to the free H_2O value of 0.69 au. Upon approaching the water molecule to the platinum atom, the $|\mathbf{M}_1|$ values of the interacting and non-interacting O−H bonds diverge: in all cases the $|\mathbf{M}_1|$ values of the interacting O−H bonds increase, down to about 3.0 Å, that is, in a region where the dispersion component of the energy is important, whereas those of the non-interacting O−H bonds remain approximately constant (*cis* isomers) or slightly decrease (*trans* isomers), see below. Obviously, the formation

dx.doi.org/10.1021/ic301512c | *Inorg. Chem.* 2013, 52, 1217−1227

Table 5. Magnitude of the Dipolar Polarization $|\mathbf{M}_1|$ (in a.u.) of the ELF Valence Basins of the Interacting Water Molecule, for the Various Pt-Complexes in the "H-ahead" Orientation Considered in This Work and for Selected Pt-Oxygen Distances (in Å)[a]

		$\|\mathbf{M}_1\|$			
	d(Pt−O)	V(O,H$_1$)	V(O,H$_2$)	V$_1$(O)	V$_2$(O)
H$_2$O		0.791	0.791	0.691	0.691
		(0.842)	(0.842)	(0.695)	(0.695)
cis-[PtCl$_2$(NH$_3$)$_2$]·H$_2$O	2.4	**0.757**	0.827	0.787	0.784
		(0.811)	(0.804)	(0.794)	0.795
	3.0	**0.867**	0.823	0.744	0.739
		(0.901)	(0.823)	(0.748)	(0.746)
	3.4	***0.860***	*0.829*	*0.732*	*0.731*
		(0.887)	*(0.838)*	*(0.722)*	*(0.726)*
	6.0	**0.812**	0.814	0.707	0.705
		(0.852)	(0.852)	(0.703)	(0.698)
trans-[PtCl$_2$(NH$_3$)$_2$]·H$_2$O	2.4	**0.783**	0.791	0.924	0.929
		(0.819)	(0.806)	(0.840)	(0.849)
	3.0	**0.863**	0.798	0.792	0.798
		(0.896)	(0.825)	(0.755)	(0.749)
	3.4	***0.857***	*0.801*	*0.755*	*0.761*
		(0.884)	*(0.833)*	*(0.727)*	*(0.728)*
	6.0	**0.812**	0.810	0.707	0.705
		(0.852)	(0.852)	(0.697)	(0.701)
cis-[Pt(OH)$_2$(NH$_3$)$_2$]·H$_2$O	2.4	**0.823**	0.806	0.769	0.772
		(0.840)	(0.798)	(0.781)	(0.783)
	3.0	**0.891**	0.827	0.737	0.737
		(0.915)	(0.829)	(0.742)	(0.738)
	3.4	***0.879***	*0.829*	*0.731*	*0.731*
		(0.897)	*(0.782)*	*(0.724)*	*(0.720)*
	6.0	**0.824**	0.813	0.708	0.703
		(0.856)	(0.852)	(0.696)	(0.695)
trans-[Pt(OH)$_2$(NH$_3$)$_2$]·H$_2$O	2.4	**0.809**	0.779	0.941	0.943
		(0.838)	(0.804)	(0.836)	(0.837)
	3.0	**0.896**	0.793	0.801	0.798
		(0.917)	(0.817)	(0.751)	(0.746)
	3.4	***0.869***	*0.802*	*0.765*	*0.763*
		(0.894)	*(0.832)*	*(0.731)*	*(0.729)*
	6.0	**0.812**	0.802	0.709	0.713
		(0.851)	(0.849)	(0.698)	(0.695)
trans-[PtCl$_2$(NH$_3$)N-*Gly*]·H$_2$O	2.4	**0.757**	0.779	0.866	0.875
	3.0	**0.858**	0.790	0.748	0.771
	3.4	***0.846***	*0.807*	*0.726*	*0.747*
	6.0	**0.803**	0.812	0.699	0.706

[a]Values in bold refer to the V(O,H) basin oriented toward the platine center. Values in italics refer to the Pt−O equilibrium distance. Values in parentheses take into account implicit solvation in water (see text). "*Gly*" means NH$_2$CH$_2$COOH.

of the dispersion-driven O−H···Pt hydrogen bond polarizes the O−H bond further. This can be related to the fact that the V(O,H$_1$) is distorted as mentioned previously, whereas the shape of the non-interacting V(O,H$_2$) basin is not modified. The enhancement of the dipolar polarization of V(O,H$_1$) is smaller for X = Cl (∼0.07 au, Figure 4a and 4b) than for X = OH (∼0.09 au, Figure 4c and 4d), which correlates nicely with the smaller charge of Pt that was found for X = Cl (Table 2). Importantly, this enhancement of dipolar polarization is nearly independent of the configuration, which is not surprising since the V(O,H$_1$) basin is directed toward the platinum atom, and the effect of the configuration is thus minor. At very short Pt···O separations (below 2.8/3.0 Å), $|\mathbf{M}_1|$ of the interacting O−H bond decreases abruptly. This decrease could be related to the further contraction and modification of the shape of the localization domain associated with the V(O,H$_1$) basin, as mentioned above (see Figure 3b, for d(Pt−O) = 2.4 Å).

In contrast, the dipolar polarization of the non-interacting O−H bond slightly decreases when d(Pt−O) decreases from 4.5 to 2.4 Å for all the *trans* complexes. For the *cis* complexes, $|\mathbf{M}_1|$ remains constant up to the energy-minimum at ∼3.4 Å, after which a slight decrease is observed. This decrease can be attributed to the particularly attractive interaction of the non-interacting O−H bond with one polar ligand (θ = 0°), whereas for the *cis*-Pt complexes the V(O,H$_2$) basin is located between both X$^-$ ligands and is therefore less influenced.

The dipolar polarization of the oxygen lone pairs (both non-interacting) increases upon approaching platinum. The increasing electric field of the platinum complex evidently repels the electrons of the non-interacting electron pairs away from the oxygen nucleus, increasing the dipolar polarization of

dx.doi.org/10.1021/ic301512c | Inorg. Chem. 2013, 52, 1217−1227

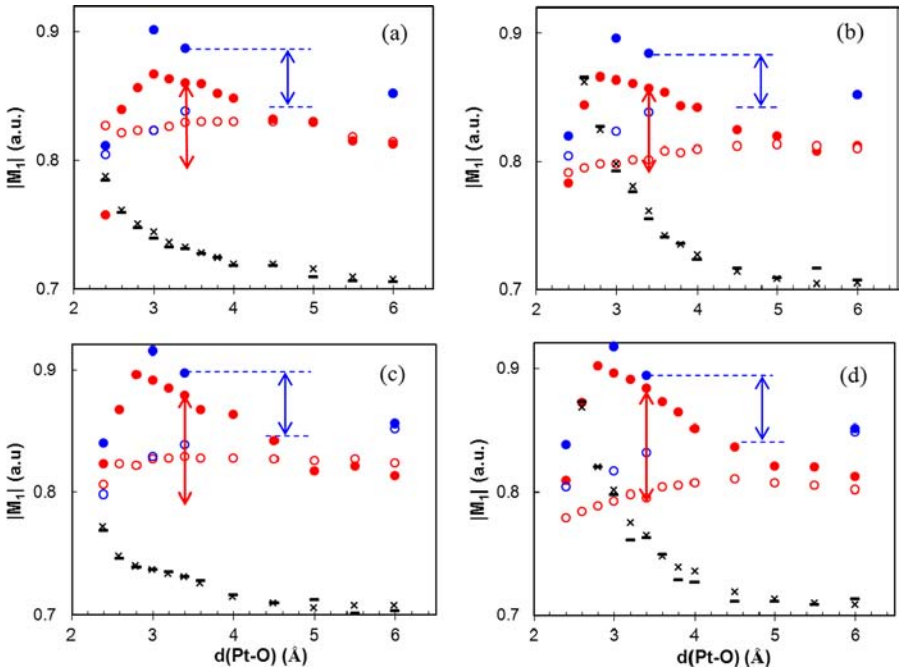

Figure 4. Magnitude of the dipolar polarization, $|\mathbf{M}_1|$, of the ELF valence basins of the water molecule, for (a) *cis*-$[PtCl_2(NH_3)_2]\cdot H_2O$, (b) *trans*-$[PtCl_2(NH_3)_2]\cdot H_2O$, (c) *cis*-$[Pt(OH)_2(NH_3)_2]\cdot H_2O$, and (d) *trans*-$[Pt(OH)_2(NH_3)_2]\cdot H_2O$ in the "H-ahead" orientation as a function of the distance between Pt and the oxygen of H_2O; (red and blue filled circles): $V(O,H_1)$, oriented toward Pt, in vacuum (red) and in water (blue); (red and blue open circles): $V(O,H_2)$, not oriented toward Pt,in vacuum (red) and in water (blue) (−) and (×): $V_1(O)$ and $V_2(O)$, in vacuum. Arrows indicate the enhancement, at the equilibrium Pt−O distance, of the dipolar polarization of the basin directed toward Pt, with respect to the value calculated for the isolated water molecule (0.791 au in vacuum and 0.842 au in water).

the lone-pairs and decreasing the dipolar polarization of the non-interacting O−H bond, as we have seen above. As one could expect, the effect on the two lone-pairs is similar.

When the effect of the polar solvent is taken into account using the implicit CPCM model, in the "H-ahead" attractive approach, all the $|M_1|$ values (associated to either the interacting or the non-interacting O−H bonds) increase with respect to those in vacuum, both for $[PtCl_2(NH_3)_2]\cdot H_2O$ and $[Pt(OH)_2(NH_3)_2]\cdot H_2O$, and independently of the configuration (Table 5 and Figure 4). The solvent-vacuum gap increases with d(Pt−O). However, this amplification is slightly larger for $[PtCl_2(NH_3)_2]$ than for $[Pt(OH)_2(NH_3)_2]$, in agreement with the larger increase of the Pt charge in the $[PtCl_2(NH_3)_2]$ complexes (see paragraph 3.2.1). The global enhancement of $|M_1|$ values observed when the axial water molecule approaches the Pt complex are thus somehow reduced when the solvent effect is taken into account, but not completely canceled.

In summary, the formation of the dispersion-driven hydrogen bond is accompanied by an increase of the dipolar polarization of the interacting O−H bond, whereas the polarization of the non-interacting O−H bond remains constant (*cis* isomers) or decreases slightly (*trans* isomers).

4. CONCLUDING REMARKS

In the present work we have carried out an extended analysis of the non-conventional H-bond that forms when an uncharged Pt(II) complex is axially approached by a water molecule. Our results, which validate the computational model initially devised,[6,7] allowed us to establish four descriptors of the non-conventional OH···Pt bond, one of the energetic nature, three of the topological one. (i) The important energetic feature appears to be the dispersion-driven character of the "H-ahead" interaction, which is modulated by the nature and the configuration of the polar ligands in vacuo. An implicit solvation model such as COSMO maintains this inverse coordination patterns as a preferential one. The equalizing of the interaction energies could be overemphasized. However, the ligand selectivity of the topological descriptors is maintained, at least in part (ii) In the "H-ahead" approach, the charge transfer between all the neutral platinum complexes and the water molecule (0.04 e at equilibrium) is of the same order of magnitude as in other classical H-bonded compounds. This charge transfer reflects a small orbital interaction which increases at shorter distances. In contrast, no charge transfer was detected for the "lone pair-ahead" approach down to 2.4 Å. The charge transfer values were not modified in the solvent. Our understanding of the "H-ahead" approach was deepened by the two following descriptors. (iii) The variations, as a function of the Pt−O distance, of the electron density and its Laplacian at the bond critical point consolidate the classification of this interaction as a H-bond but also point out the influence of the nature of the ligands in vacuo as well as in the solvent. (iv) The "H-ahead" approach is accompanied by an increase of the dipolar polarization of the interacting O−H bond. Conversely the polarization of the non-interacting O−H bond decreases slightly. Thus this descriptor, which has never been applied in this context, clearly differentiates the interacting OH bond from the non-interacting one. It is noteworthy that the variations of the dipolar polarization and of the Laplacian are similar, the position of their maxima being close to each other. However, the ELF descriptor is more sensitive to the influence of the ligands. As expected, the dipolar polarization of the OH bonds increases in the aqueous medium, but the ligand selectivity is retained. This descriptor could be used to characterize other (peculiar) interactions in inorganic H-bonded compounds.

dx.doi.org/10.1021/ic301512c | *Inorg. Chem.* 2013, 52, 1217−1227

A further study of this non-conventional H-bond using the recently developed NCI (Non-Covalent Interactions) approach,[56,57] which is based on the electron density and its reduced gradients and allows visualization of both attractive (van der Waals and hydrogen bonds) and repulsive interactions, is underway in our laboratories.

■ ASSOCIATED CONTENT

Supporting Information

Further details are given in Figures S1−S2 and Table S1. This material is available free of charge via the Internet at http://pubs.acs.org.

■ AUTHOR INFORMATION

Corresponding Author

*E-mail: jb@lct.jussieu.fr.

Notes

The authors declare no competing financial interest.

■ REFERENCES

(1) Elizondo-Riojas, M.-A.; Kozelka, J. *J. Mol. Biol.* **2001**, *314*, 1227−1243 , and references therein.
(2) Bhattacharyya, D.; Ramachandran, S.; Sharma, S.; Pathmasiri, W.; King, C. L.; Baskerville-Abraham, I.; Boysen, G.; Swenberg, J. A.; Campbell, S. L.; Dokholyan, N. V.; C. S., G. *PLoS One* **2011**, *6*, e23582.
(3) Carloni, P.; Sprik, M.; Andreoni, W. *J. Phys. Chem.* **2000**, *104*, 823−835.
(4) Truflandier, L. A.; Autschbach, J. *J. Am. Chem. Soc.* **2010**, *132*, 3472−3483.
(5) Truflandier, L. A.; Sutter, K.; Autschbach, J. *Inorg. Chem.* **2011**, *50*, 1723−1732.
(6) Kozelka, J.; Bergès, J.; Attias, R.; Fraitag, J. *Angew. Chem., Int. Ed. Engl.* **2000**, *39*, 198−201.
(7) Rizzato, S.; Bergès, J.; Mason, S. A.; Albinati, A.; Kozelka, J. *Angew. Chem., Int. Ed.* **2010**, *49*, 7440−7443.
(8) Vidossich, P.; Ortuno, M. A.; Ujaque, G.; Lledos, A. *ChemPhysChem* **2011**, *12*, 1666−1668.
(9) Bergès, J.; Caillet, J.; Langlet, J.; Kozelka, J. *Chem. Phys. Lett.* **2001**, *344*, 573−577.
(10) Kumar, M.; Kozlowski, P. M. *Angew. Chem., Int. Ed.* **2011**, *123*, 8861−8864.
(11) Kumar, M.; Kumar, N.; Hirao, H.; Kozlowski, P. M. *Inorg. Chem.* **2012**, *51*, 5533−5538.
(12) Kumar, M.; Hirao, H.; Kozlowski, P. M. *J. Biol. Inorg. Chem.* **2012**, *17*, 1107−1121.
(13) Coste, F.; Malinge, J.-M.; Serre, L.; Shepard, W.; Roth, M.; Leng, M.; Zelwer, C. *Nucleic Acids Res.* **1999**, *27*, 1837−1846.
(14) Fedoce Lopes, J.; Stroele de A. Menezes, V.; Duarte, H. A.; Rocha, W. R.; De Almeida, W. B.; Dos Santos, H. F. *J. Phys. Chem. B* **2006**, *110*, 12047−12054.
(15) Fu, C.-F.; Tian, S.-X. *J. Chem. Phys.* **2010**, *132*, 174507.
(16) Baidina, I. A.; Podberezskaya, N. V.; Borisov, S. V.; Shestakova, N. A.; Kyklina, U. F.; Mal'chikov, G. D. *Zh. Strukt. Khim.* **1979**, *20*, 548−551.
(17) Baidina, I. A.; Podberezskaya, N. V.; Krylova, L. F.; Borisov, S. V. *J. Struct. Chem.* **1981**, *22*, 463−465.
(18) Beret, E. C.; Martínez, J. M.; Pappalardo, R. R.; Sánchez Marcos, E.; Doltsinis, N. L.; Marx, D. *J. Chem. Theory Comput.* **2008**, *4*, 2108−2121.
(19) Beret, E. C.; Pappalardo, R. R.; Doltsinis, N. L.; Marx, D.; Sánchez Marcos, E. *ChemPhysChem* **2008**, *9*, 237−240.
(20) Fedoce Lopes, J.; Da Silva, J. C. S.; Rocha, W. R.; De Almeida, W. B.; Dos Santos, H. F. *J. Chem. Theory Comput.* **2011**, *10*, 371−391.
(21) Vinje, J.; Sletten, E.; Kozelka, J. *Chem.—Eur. J.* **2005**, *11*, 3863−3871.
(22) Burda, J. V.; Zeizinger, M.; Sponer, J.; Leszynski, J. *J. Chem. Phys.* **2000**, *113*, 2224−2232.
(23) Zimmermann, T.; Burda, J. V. *Interdiscip. Sci.Comput. Life Sci.* **2010**, *2*, 98−114.
(24) Pilmé, J.; Piquemal, J.-P. *J. Comput. Chem.* **2008**, *29*, 1440−1449.
(25) Popelier, P. In *Structure and Bonding*; Wales, D. J., Ed.;Springer-Verlag: Berlin, Germany, 2005; Vol. *115*, pp 1−56.
(26) Popelier, P. L. A.; Brémond, E. A. G. *Int. J. Quantum Chem.* **2009**, *109*, 2542.
(27) Bader, R. F. W. *Atoms in Molecules: A Quantum Theory*; Oxford Univ. Press: Oxford, U.K., 1990.
(28) Becke, D.; Edgecombe, K. E. *J. Chem. Phys.* **1990**, *92*, 5397.
(29) Feixas, F.; Matito, E.; Duran, M.; Sola, M.; Silvi, B. *J. Chem. Theory Comput.* **2010**, *6*, 2736−2740.
(30) Silvi, B.; Savin, A. *Nature* **1994**, *371*, 683.
(31) Silvi, B. *J. Mol. Struct.* **2002**, *614*, 3−10.
(32) Bader, R. F. W.; Larouche, A.; Gatti, C.; Caroll, M. T.; Dougall, P. J.; Wiberg, K. B. *J. Chem. Phys.* **1987**, *87*, 1142.
(33) Boys, S. F.; Bernardi, F. *Mol. Phys.* **1970**, *19*, 553−566.
(34) van Duijneveldt, F. B.; van Duijneveldt-van de Rijdt, J. G. C. M.; van Lenthe, J. H. *Chem. Rev.* **1994**, *94*, 1873−1885.
(35) Andrae, D.; Häussermann, U.; Dolg, M.; Stoll, H.; Preuss, H. *Theor. Chim. Acta* **1990**, *77*, 123−141.
(36) Kozelka, J.; Bergès, J. *J. Chim. Phys.* **1998**, *95*, 2226−2240.
(37) Langlet, J.; Bergès, J.; Caillet, J.; Kozelka, J. *Theor. Chem. Acc.* **2000**, *104*, 247−251.
(38) Chalasinski, G.; Szczesniak, M. M. *Chem. Rev.* **1994**, *94*, 1723−1765.
(39) He, X.; Fusti-Molnar, L.; Cui, G.; Merz, K. M., Jr. *J. Phys. Chem. B.* **2009**, *113*, 5290−5300.
(40) Frisch, M. J.; Trucks, G. W.; Schlegel, H. B.; Scuseria, G. E.; Robb, M. A.; Cheeseman, J. R.; Montgomery, Jr., J. A.; Vreven, T.; Kudin, K. N.; Burant, J. C.; Millam, J. M.; Iyengar, S. S.; Tomasi, J.; Barone, V.; Mennucci, B.; Cossi, M.; Scalmani, G.; Rega, N.; Petersson, G. A.; Nakatsuji, H.; Hada, M.; Ehara, M.; Toyota, K.; Fukuda, R.; Hasegawa, J.; Ishida, M.; Nakajima, T.; Honda, Y.; Kitao, O.; Nakai, H.; Klene, M.; Li, X.; Knox, J. E.; Hratchian, H. P.; Cross, J. B.; Bakken, V.; Adamo, C.; Jaramillo, J.; Gomperts, R.; Stratmann, R. E.; Yazyev, O.; Austin, A. J.; Cammi, R.; Pomelli, C.; Ochterski, J. W.; Ayala, P. Y.; Morokuma, K.; Voth, G. A.; Salvador, P.; Dannenberg, J. J.; Zakrzewski, V. G.; Dapprich, S.; Daniels, A. D.; Strain, M. C.; Farkas, O.; Malick, D. K.; Rabuck, A. D.; Raghavachari, K.; Foresman, J. B.; Ortiz, J. V.; Cui, Q.; Baboul, A. G.; Clifford, S.; Cioslowski, J.; Stefanov, B. B.; Liu, G.; Liashenko, A.; Piskorz, P.; Komaromi, I.; Martin, R. L.; Fox, D. J.; Keith, T.; Al-Laham, M. A.; Peng, C. Y.; Nanayakkara, A.; Challacombe, M.; Gill, P. M. W.; Johnson, B.; Chen, W.; Wong, M. W.; Gonzalez, C.; and Pople, J. A. *Gaussian 03*, Revision B.02; Gaussian, Inc.: Pittsburgh, PA, 2004.
(41) Pilmé, J.; Kozlowski, D. *J. Comput. Chem.* **2011**, *32*, 3207−3217.
(42) The TopChem90 package is freely available on: http://www.lct.jussieu.fr/pagesperso/pilme/topchempage.html.
(43) Noury, S.; Krokidis, X.; Fuster, F.; Silvi, B. *Comput. Chem.* **1999**, *23*, 597.
(44) Flukiger, P.; Luthi, H. P.; Portman, S.; Weber, J. *Molekel*; Swiss Center for Scientific Computing: Manno, Switzerland, 2000−2002.
(45) Fedoce Lopes, J.; Rocha, W. R.; Dos Santos, H. F.; De Almeida, W. B. *J. Chem. Phys.* **2008**, *128*, 165103.
(46) Fedoce Lopes, J.; Rocha, W. R.; Dos Santos, H. F.; De Almeida, W. B. *J. Braz. Chem.Soc.* **2010**, *21*, 887−96.
(47) Martín Pendás, A.; Blanco, M. A.; Francisco, E. *J. Chem. Phys.* **2006**, *125*, 184112.
(48) Devereux, M.; Popelier, P. L. A. *J. Phys. Chem. A* **2007**, *111*, 1536−1544.
(49) Li, Y.; Zhang, G.; Chen, D. *Mol. Phys.* **2012**, *110*, 179−184.
(50) Popelier, P. L. A.; Logothetis, G. *J. Organomet. Chem.* **1998**, *555*, 101−111.
(51) Weinhold, F. In *Encyclopedia of Computational Chemistry*; Schleyer, P. V. R., Allinger, N. L., Gasteiger, T., Clark, J., Kollman, P.

A., Schaefer, H. F., III, Schreiner, P. R., Eds.; Wiley: Chichester, U.K., 1998; Vol. 3, p 1792.
(52) (a) Koch, U.; Popelier, P. L. A. *J. Phys. Chem.* **1995**, *99*, 9747. (b) Popelier, P. L. A. *J. Phys. Chem. A* **1998**, *102*, 1873.
(53) (a) Gálvez, O.; Gómez, P. C.; Pacios, L. F. *J. Chem. Phys.* **2001**, *115*, 11166. (b) Woodford, J. N. *J. Phys. Chem. A* **2007**, *111*, 8519−8530.
(54) Pacios, L. F. *J. Phys. Chem. A* **2004**, *108*, 1177−1188.
(55) Gillespie, R. J. *Molecular Geometry*; Van Nostrand Reinhold: London, U.K., 1972.
(56) Contreras-García, J.; Johnson, E. R.; Keinan, S.; Chaudret, R.; Piquemal, J.-P.; Beratan, D. N.; Yang, W. *J. Am. Chem. Soc.* **2010**, *132*, 6498−6506.
(57) Contreras-García, J.; Yang, W. *J. Phys. Chem. A* **2011**, *115*, 12983−12990.

dx.doi.org/10.1021/ic301512c | *Inorg. Chem.* 2013, 52, 1217−1227